ISSN: 0976-9102 (ONLINE)
DOI: 10.21917/ijivp.2020.0310

LOG-GABOR BINARIZED STATISTICAL DESCRIPTOR FOR FINGER KNUCKLE PRINT RECOGNITION SYSTEM

Mourad Chaa
Department of New Technologies of Information and Communication, Ouargla University, Algeria

Abstract

This paper proposes a new local image descriptor for Finger Knuckle Print Recognition Systems (FKPRS), named Log-Gabor Binarized Statistical Image Features descriptor (LGBSIF). The idea of LGBSIF is based on the image Log-Gabor wavelet representation and the Binarized Statistical Image Features (BSIF). Initially, the Region of Interest (ROI) of the FKP images are analyzed with a 1D Log-Gabor wavelet to extract the preliminary features that are presented by both the real and imaginary parts of the filtered image. The main motive of the LGBSIF is to enhance the Log-Gabor real and imaginary features by applying the BSIF coding method. Secondly, histograms extracted from the encoded real and imaginary images respectively are concatenated in one large feature vector. Thirdly, the PCA+LDA technique is used to reduce the dimensionality of this feature and enhance its discriminatory power. Finally, the Nearest Neighbor Classifier that uses the Cosine distance is employed for the matching process. The evaluation of the performance of the proposed system is done on the Poly-U FKP database. However, the experimental results have shown that the proposed system achieves better results than other state-of-the-art systems and confirmed the tenacity of the proposed descriptor. Further, the results also prove that the performance efficiency of the introduced system in terms of recognition rate (Rank1) and equal error rate (EER) are 100% and 0% for both modes of identification and verification respectively.

Keywords:

Biometric, Local Descriptor, Wavelet, Dimensionality Reduction, Classification

1. INTRODUCTION

Biometrics is the branch of science which deals with automated methods of recognizing a person based on physiological or behavioral traits. During the past years, researchers have investigated and developed a number of biometric modalities, including voice recognition, facial recognition, fingerprint, iris recognition, palmprint and FKP [1]. Recently, researchers have proved that patterns taken from skin folds and creases extracted from the outer finger knuckle surface are highly unique and can be used as distinctive biometric identifiers [2]. To validate this there are some advantages if they are compared with a fingerprint counterpart as shown in Fig.1. For example, the acquisition of the surfaces data of finger-knuckles is relatively simple and cost-effective using low-resolution cameras.

Secondly, FKP-based access systems can be used under various environmental conditions such as indoor and outdoor. Thirdly, FKP features taken from adults usually remain stable over time and ageing. Finally, a FKP-based biometric recognition system is very reliable [2].

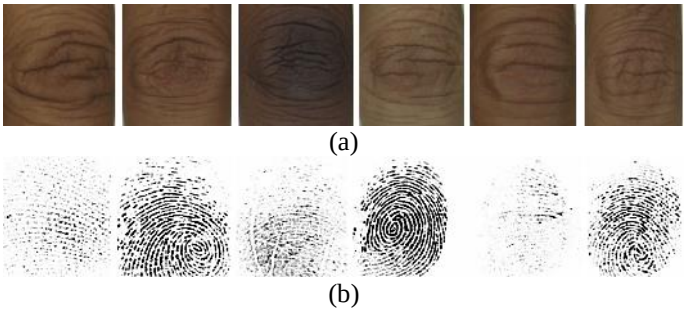

(a) (b)

Fig.1. Knuckle print and Fingerprint (a) Knuckle print and (b) Fingerprint

However, biometric system can be deployed for various applications, such as biometric access control system, video surveillance, airport checking, computer or mobile device systems, etc. [1]. Many research papers and studies on the FKP are available by simply googling on the web. Within this plethora of works, recent surveys and tutorials have been published, sketching the state-of-the-art methods in the field [2]-[6]. In [2], Zhang et al. have combined both local and global in the feature extraction stage where the local orientation is extracted by a set of Gabor filters while the Fourier coefficients are taken as a global feature. In [3], Shariatmadar and Faez introduced an approach to personal recognition using FKP where the extracted features of intensity and Gabor images of each FKP have been combined to each other. Zeinali et al. [4] have proposed a system for FKP recognition based on Directional Filter Bank for feature extraction. Then dimensionality of the extracted feature has been reduced by using Linear Discriminate Analysis (LDA). Chaa et al. [5] presented a novel method to extract the optimal discriminant features from FKP images. However, the 1D-Log Gabor filter, the Gabor filter bank and LDA have been used. First of all, the ROI of FKP images have been analyzed with a 1D Log-Gabor wavelet to extract the preliminary feature. Then, to select only the discriminative features of FKP image a Gabor filter bank has been applied on this preliminary feature.

Finally, the LDA technique has been used to reduce the dimensionality. For matching process, the cosine Mahalanobis distance has been used. The 1D Log-Gabor transform has been successfully used in texture analysis, image processing, and computer vision. In most cases, solely the magnitude or phase information of the Log-Gabor transform is taken into account. However, the complementary effect taken from the real and imaginary information for an image-feature extraction problem has not been systematically examined in the existing works except in the work [6]. However, each image FKP has been represented by the real and the imaginary feature vector. Then, these vectors have been binarized for extracting binary response.

The main objective of this work is to provide a good system to recognize people using their FKP. Firstly, 1D-Log Gabor filter

has been applied on the ROI for each FKP image. However, the use of Log-Gabor filter is to remove the noise from FKP images and is also extensively used to extract texture information from these images. As the BSIF is very robust for gray scale, rotation variations and uneven illumination problem, subsequently, each real and imaginary part of each filtered image is encoded using BSIF coding method to ensure that the FKP features are extracted more effectively.

In the second stage, the histograms (feature vectors) are extracted from the encoded real and imaginary images. Then these feature vectors are concatenated to produce a single large feature vector. In fact, coupling the Log-Gabor filter and BSIF allows extracting a set of features that can reflect the local information. In the third stage the popular subspace projection method called PCA+LDA for FKP recognition is applied for the dimensionality reduction of large feature vectors of all users before classifying the FKP images.

The main objective of dimensionality reduction is executed by projecting the feature vectors onto a lower dimensional space while still keeping the most distinguishing features which in turn reduce the computational complexity of the system.

The remaining parts of this paper is organized as follows: section 2 presents an overview of the proposed system. Section 3 discusses the feature extraction method along with a brief overview of the Gabor filter and LDA technique. Section 4 focalizes on the matching process used in our system. In section 5, the experimental results are discussed and commented. Section 6 contains the conclusion and recommendations for further works in the context of this paper.

2. PROPOSED FKP RECOGNITION SYSTEM

An FKP recognition system is a system for recognizing persons using Finger Knuckle Print modality. Mainly, it consists of different main steps. First, we started by acquiring the biometric data of the individual person. Followed by extracting a set of characteristics from the acquired biometric data, then comparing between these characteristics and the features stored in the database. In fact, there are two phases: the training phase and the test phase (see Fig.2).

During the training phase, the biometric data of a person belonging to the system has been stored in a database. Typically, biometric data acquired by the capture module are processed by the feature extraction module to extract feature vectors that are characteristic of each individual. During the test phase, the acquired biometric data test per person is compared with the data stored in database in the matching module. The identity of the person is determined by the decision module as depicted in Fig.3. Fig.3 is the diagram of the proposed LGBSIF descriptor system based on FKP modality using 1D Log-Gabor filter, wherein the BSIF Descriptor, and the PCA+LDA technique are clearly illustrated.

The 1D-Log Gabor filter has been employed to generate the preliminary feature using the Real Image (RI) and Imaginary Image (II) of the filtered image. To enhance the Log-Gabor real and imaginary feature, the BSIF coding method is applied. Subsequently, the histograms extracted from the encoded real and imaginary images are respectively merged to produce a single large feature vector. This process is followed by dimensionality reduction of this feature vector using PCA+LDA technique. Finally, the nearest neighbor classifier is used for classifying the individuals. This classifier uses the cosine distance for the matching stage.

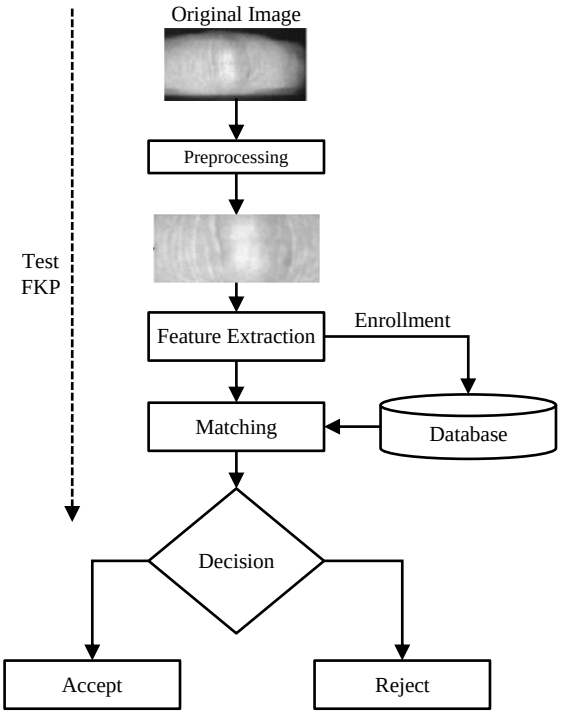

Fig.2. Diagram for the person recognition using FKP based on LGBSIF

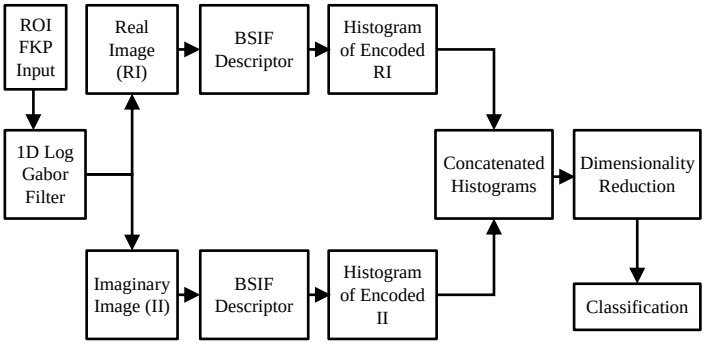

Fig.3. Log-Gabor Binarized Statistical Image Features descriptor (LGBSIF)

The following are the detailed steps furnished by [7] for extracting the region of interest (ROI) of FKP:

- First, a Gaussian smoothing operation is applied to the original image, and then the smoothed image is down-sampled to 150 dpi.
- The X-axis of the coordinate system fitted is determined from the bottom boundary of the finger to ensure the easy extraction of the bottom boundary of the finger using a canny edge detector.
- The Y-axis of the coordinate system is determined by applying a canny edge detector on the cropped sub-image that is extracted from the image's original base on X-axis.
- The convex direction coding scheme is deciphered.

- Finally, the ROI system is extracted.
- In Fig.4, the rectangle indicates the area of the ROI that will be extracted.

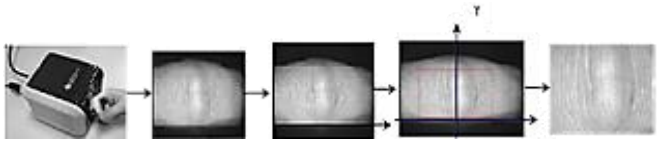

Fig.4. Steps of extraction of FKP ROI image

2.1 FEATURE EXTRACTION USING LGBSIF DESCRIPTOR

2.1.1 Log-Gabor Filter:

Gabor filter has been used as feature extractor in image analysis and computer vision. However, one of the disadvantage of a Gabor filter is that the even symmetric filter will have a DC component whenever the bandwidth is larger than one octave. Gabor filters are not optimal if one is seeking broad spectral information with maximal spatial localization. To overcome this weakness, a Log-Gabor filter proposed by Field [8] has been used to eliminate the DC component, thus this filter is allowed to produce zero DC components for any band width. Log-Gabor filter can be constructed with arbitrary bandwidth which can be optimized to produce a filter with minimal spatial extent. The frequency response of a Log-Gabor filter is given by:

$$G(f) = \exp\left[\frac{-\left(\log\left(\frac{f}{f_0}\right)\right)}{2\left(\log\left(\frac{\sigma}{f}\right)^2\right)}\right] \quad (1)$$

where f_0 represents the centre frequency and σ gives the bandwidth of filter. The parameters of Log-Gabor filter were empirically selected as f_0 = 0.5 and σ = 0.0556. Each row of the FKP ROI image (110×220 pixels) is filtered using 1D-Log-Gabor filter. The result will be 110×220 arrays of complex numbers. The real and imaginary parts of this array are computed as shown in Fig.5.

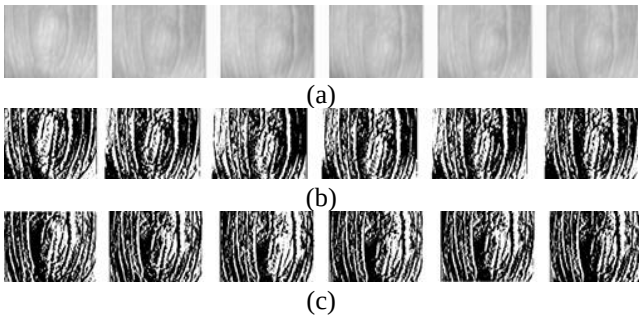

(a)

(b)

(c)

Fig.5. (a) Sample of the FKP ROI images (b) Real parts (c) Imaginary parts

2.1.2 Binarized Statistical Image Features:

A Binarized Statistical Image Feature (BSIF) is a recent textural local descriptor that is based on a set of filters of fixed size which describe the neighborhood configuration of the central pixel. When BSIF filters a given image X of size $m \times n$ with a set of filters $\varphi_i^{k\times k}$, then the responses are binarized and obtained as follows [9]:

$$r_i = \sum_{m,n} \phi_i^{k\times k} X(m,n) \quad (2)$$

where,

$\varphi_i^{k\times k}$ is a linear filter of size k and $i=\{1,2,\ldots,n\}$ denotes the number of statistically independent filters whose response can be computed together and binarized to obtain the binary string as follows [9]:

$$b_i = \begin{cases} 1 & if\ r_i > 0 \\ 0 & otherwise \end{cases} \quad (3)$$

Finally, the BSIF features are obtained as the histogram of pixel's binary codes that can effectively characterize the texture components in the FKP image. There are two important factors in BSIF descriptor namely: the filter size k and the filter length (n). The corresponding BSIF code depth and intensity images are shown in Fig.6. The Fig.6(a) indicates the input ROI FKP image. The Fig.6(b) shows the learned BSIF filter with a size 11×11 and of length 12. The Fig.6(c) shows the results of the individual convolution of the ROI FKP image with BSIF filter. The Fig.6(d) shows the final BSIF feature encoded.

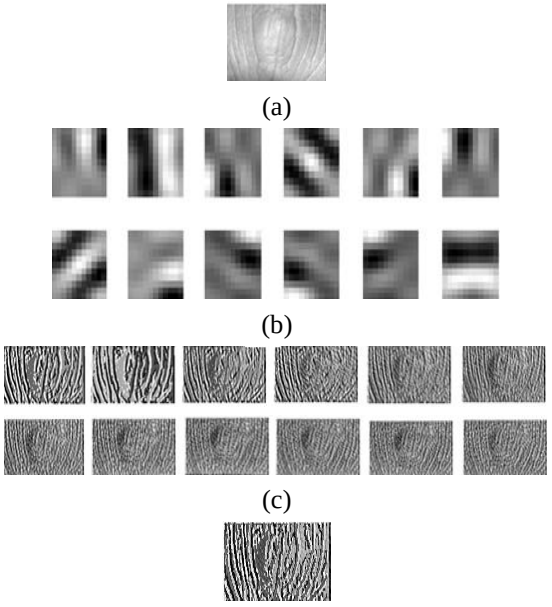

(a)

(b)

(c)

(d)

Fig.6. (a) Sample of the FKP ROI image (b) BSIF filter with a size 11×11 and of length 12 (c) BSIF features (d) final BSIF

2.2 DIMENSIONALITY REDUCTION

In the next step, histograms extracted from the encoded real and imaginary images using BSIF descriptor are concatenated to produce a large feature vector. The large features extracted from the previous stage have high dimensions and it is difficult to evaluate them. Principal Component Analysis (PCA) is a widely used and simple method for dimensionality reduction which does not take into account the separability of the classes [10]. To achieve a much-improved separability of feature subspace, LDA [11] can be deployed resulting in attractive performances for

recognition tasks although LDA still assumes a common covariance matrix among the classes which violate the normality principle.

In this paper, PCA algorithm is applied to reduce the dimensionality of large features. Then LDA algorithm is applied on PCA weights to increase the separability between classes. Using this method on our data, 164 most important features are selected.

2.3 MATCHING MODULE AND NORMALIZATION SCORE

In our work we use four distances metric. Given two vectors $V_i = v_1, v_2,\ldots, v_n$ and $Y_j = y, y_2,\ldots, y_n$ the Euclidean distance (Eu) is obtained by the following relation:

$$d_{Eu}\left(V_i, Y_j\right) = \sqrt{\left(V_i - Y_j\right)^T \left(V_i - Y_j\right)} \quad (4)$$

The Mahalanobis distance (Ma) is given by the Eq.(5), where C is the covariance matrix:

$$d_{MA}\left(V_i, Y_j\right) = \left(V_i - Y_j\right)^T C^{-1} \left(V_i - Y_j\right) \quad (5)$$

The City block distance (Ctb) is given by:

$$d_{Ctb}\left(V_i, Y_j\right) = \sum_{q=1}^{n} \left|V_{iq} - Y_{jq}\right| \quad (6)$$

The Cosine distance (Cos) is given by:

$$d_{\cos}\left(V_i, Y_j\right) = \left(1 - \frac{V_i Y_j^T}{\sqrt{\left(V_i V_i^T\right)\ \left(Y_i Y_j^T\right)}}\right) \quad (7)$$

Therefore, prior to finding the decision, a method named Min-Max normalization scheme was employed to transform the score vectors computed. Given a set of matching scores X_k, where k=1, 2,⋯,n. The normalization scores are taken as:

$$X_k^{'} = \frac{X_k + \min}{\max - \min} \quad (8)$$

where X_k' represents the normalized scores.

2.4 COMPUTATIONAL COMPLEXITY OF THE LGBSIF ALGORITHM

To examine the computational complexity of the proposed LGBSIF algorithm, we will study the Log-Gabor filter, the BSIF descriptor and the PCA+LDA methods separately. Furthermore, mainly the computational complexity of the LGBSIF method falls into the training process, so the focus will be on this part of the method.

According to the authors [12], the computational complexity of each BSIF is $O(p^2)$ where p^2 is the number of pixels of the input image. For a $P\times P$ image and $F\times F$ filter, the first results are obtained in a computational complexity of $O(F^2)$ for each pixel of the input image. Thus, for the whole image the multiplications or additions of $O(P^2F^2)$ are required. If we suppose that the available training set includes q images, the total computational complexity for executing BSIF filtering process in the spatial domain is $O(qP^2F^2)$. However, computational complexity relatively is dependent on several parameters such as the number of the BSIF filter, the size of the image to be filtered, number of image in training set as well as the size of filter.

The PCA+LDA algorithm requires $O(q^3)$ operations [13] where q refers to the number of training samples. Once the PCA+LDA model is done, each of the training samples is projected into the PCA+LDA subspace a procedure that requires [13], $O(qNM)$ operations, where M and N are the number of elements and the number of classes in the training data respectively.

3. EXPERIMENTAL RESULTS AND DISCUSSION

3.1 DATABASE

An FKP database obtained from Hong Kong polytechnic university (PolyU) is used for evaluating the proposed system. This database contains 7920 images obtained from 165 persons including 125 males and 40 females. Among them, 143 subjects are 20∼30 years old and the others are 30∼50 years old. This collection of images was dealt in two sessions, with 48 different FKP images of each person. Four finger types of each person are collected. Which are: Left Index Fingers (LIF), Left Middle Fingers (LMF), Right Index Fingers (RIF) and Right Middle Fingers (RMF). Each finger type provides 12 images (6 images in each session). However, the total number of images, for each finger type, is 1980 images.

Experiment 1: In experiment 1, the BSIF descriptor has been applied directly on FKP image without Log-Gabor filter in order to select the best BSIF parameters. However, in this experiment, we took images collected from the first session as the gallery set and images collected from the second session as the probe set of each finger type. It has been noted that the parameters, the filter size k and the filter length n, have a great influence on the performance of the proposed system. Thus, several tests are performed on both the FKP identification and the verification of the results is illustrated in Table.1.

Table.1. Best BSIF parameters

Parameters		**LMF**		**LIF**		**RIF**		**RMF**	
k	***n***	**Rank-1**	**EER**	**Rank-1**	**EER**	**Rank-1**	**EER**	**Rank-1**	**EER**
17×17	12	98.08	0.30	97.88	0.30	96.57	0.51	98.08	0.20
17×17	11	95.56	0.89	95.66	0.91	95.05	0.91	95.96	0.51
17×17	10	87.98	2.02	87.68	2.22	87.27	3.03	89.60	2.21
17×17	9	83.54	2.93	83.94	3.23	81.11	4.76	84.04	3.64
17×17	8	79.49	4.27	81.41	4.04	77.27	5.13	77.88	5.13
15×15	12	98.28	0.22	98.38	0.30	97.58	0.61	98.89	0.10
15×15	11	96.36	0.81	96.97	0.59	95.35	0.79	96.57	0.38
15×15	10	89.80	2.02	89.29	2.02	88.79	2.22	89.70	1.54
15×15	9	84.65	3.12	81.72	3.13	81.62	4.14	85.15	2.53
15×15	8	80.81	3.74	81.82	4.15	82.12	3.52	80.81	3.64
13×13	12	98.08	0.20	98.48	0.30	97.27	0.40	98.59	0.20

13×13	11	96.46	0.41	97.07	0.51	96.16	0.61	97.37	0.51
13×13	10	91.62	1.21	90.61	1.62	87.88	2.41	90.40	2.12
13×13	9	84.95	2.44	86.16	2.52	84.14	3.84	85.45	2.83
13×13	8	82.63	3.85	83.94	3.13	82.93	3.54	84.14	3.44
11×11	12	98.79	0.20	98.89	0.20	97.68	0.40	98.99	0.10
11×11	11	96.46	0.30	97.37	0.40	96.06	0.81	97.17	0.30
11×11	10	90.51	1.92	91.52	1.72	87.68	2.42	92.53	1.62
11×11	9	85.96	2.63	86.97	2.83	83.74	3.94	86.06	2.92
11×11	8	85.35	2.93	85.45	2.91	83.84	3.33	88.79	2.31
9×9	12	98.48	0.30	98.89	0.18	97.68	0.40	98.79	0.40
9×9	11	96.97	0.69	97.68	0.38	94.44	0.99	97.07	0.51
9×9	10	89.70	1.70	87.58	1.92	86.06	2.85	89.49	1.92
9×9	9	85.76	2.22	85.66	2.10	81.72	3.94	87.98	2.61
9×9	8	86.26	3.02	87.78	2.51	83.33	3.85	88.38	2.53
7×7	12	96.46	0.51	97.37	0.38	95.86	0.62	97.17	0.61
7×7	11	94.85	0.81	96.16	0.71	92.93	1.01	95.15	1.01
7×7	10	84.14	3.34	83.13	2.83	80.91	3.33	84.14	84.14
7×7	9	81.82	3.93	77.37	4.05	78.08	4.75	79.60	4.34
7×7	8	85.25	3.33	81.21	3.52	79.19	3.94	84.95	3.74
5×5	12	88.18	2.32	89.39	1.41	87.47	2.63	89.90	1.90
5×5	11	82.12	3.21	80.81	3.23	80.30	3.45	83.94	3.33
5×5	10	58.69	8.48	57.17	8.44	59.29	8.38	64.24	7.78
5×5	9	60.91	8.92	55.35	8.36	58.79	9.07	60.51	8.49
5×5	8	69.09	7.27	65.86	7.07	66.57	7.98	67.78	6.66

*Rank and EER in %

The results of the identification experiment are provided in the form of recognition rate, wherein Rank-1 is calculated as follows:

$$Rank-1=\frac{N_i}{N}\times 100(\%) \quad (9)$$

where N_i denotes the number of images successfully assigned to the right identity and N stands for the total number of images subjected to the identification process. Results are provided in the form of Error Equal Rate (EER) when FAR (False Accept Rate) = FRR (False Reject Rate) towards verifying the accuracy of the experiment.

As disclosed by Table.1, it is observed that the performance increases with the length n of the BSIF descriptor. The parameters corresponding to the best performance have been chosen. These parameters are as follows: For LMF and RMF modalities: k=11 and n=12 and for LIF and RIF modalities: k=9 and n=12. However, these parameters have been fixed and used as an input in the simulation of Experiment 2.

Experiment 2: In experiment 2, the Log-Gabor filter has been used as shown in Fig.3. Then the best BSIF parameters have been fixed and the parameters of Log-Gabor filter have been selected empirically such as: f_0 =0.5 and σ =0.005. These parameters have been used in all computation steps. Thus, several tests have been performed and the results are illustrated in Table.2.

Table.2. Results of the proposed method

	Identification	**Verification**		
	Rank-1	**EER**	**VR@1%FAR**	**VR@0.1%FAR**
LMF	99.60%	0.10 %	100.00%	99.90%
LIF	99.19%	0.10%	100.00%	99.90%
RIF	99.39%	0.11%	100.00%	99.90%
RMF	100.00%	0.00%	100.00%	100.00%

From the Table.1 and Table.2, it is clear that, LGBSIF performs better than BSIF. Also, the proposed system can achieve higher accuracy on the RMF modality compared to the other finger types LIF, RIF and LMF. So, in this case, a recognition rate of Rank-1 equals 100% for identification mode and EER=0.00% for verification mode. The performance, in the case of identification mode, are presented in term of CMC curves (Cumulative Match Characteristic) and presented in terms of ROC curve (Receiver Operating Characteristic) for verification mode.

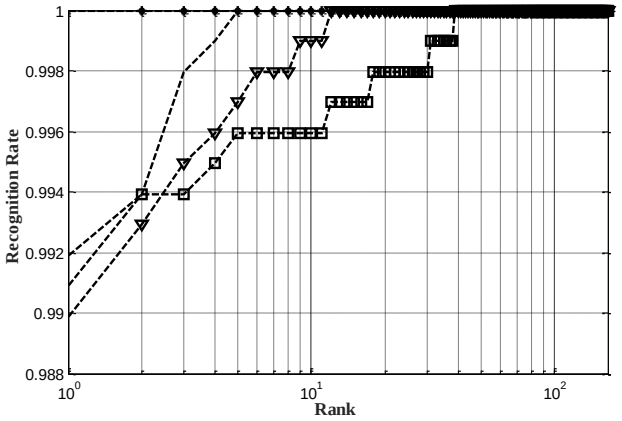

Fig.7. Comparison between different methods (CMC curve)

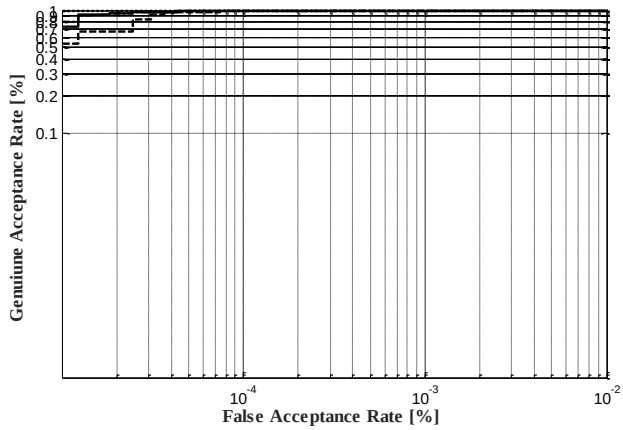

Fig.8. Comparison between different methods (ROC curve)

Also, this section provides a comparison study between different features obtained from the encoded real part (Real part+BSIF+PCA+LDA), the encoded imaginary part (Imaginary part+BSIF+PCA+LDA), the encoded FKP ROI Image

(BSIF+PCA+LDA. i.e. without 1D-Log-Gabor filter) and the proposed method (LGBSIF) using RMF modality for both identification mode (see Fig.7 CMC curve) and verification mode (see Fig.8 ROC curves).

It is clear from these curves that, when the features of the proposed method are used, the performance is higher. As evident from Fig.9 and Fig.10, the cosine distances have achieved the best performance for LGBSIF among the measures of other distances (Ma, Ctb and Eu).

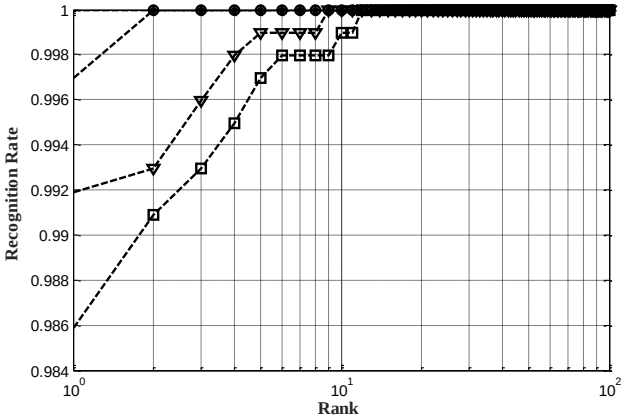

Fig.9. Comparison between different distances (CMC curve)

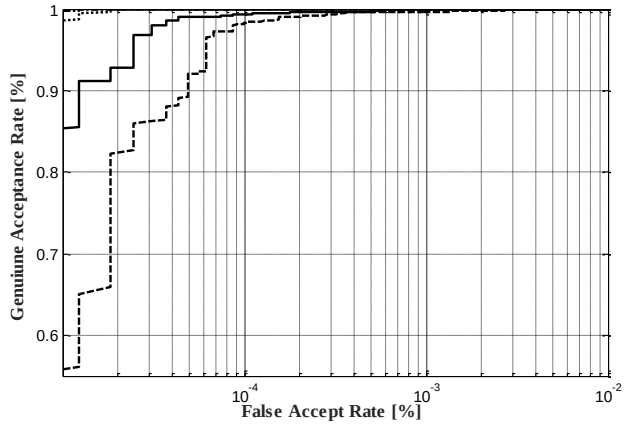

Fig.10. Comparison between different distances (CMC curve)

Finally, for proving the importance of the introduced method, a comparison study of the proposed unimodal system and some originally works in the literature was made and the obtained results are given in Table.3, which clearly establishes that the proposed method outperforms the other methods deployed for comparison. Further, as indicated by Table.3, it is inferred from the best results displayed in bold font that the proposed system has achieved better results than the other state-of-the-art systems.

Table.3. Comparative of the proposed method with the existing approaches

Reference	Year	Rank-1				EER			
		LMF	LIF	RIF	RMF	LMF	LIF	RIF	RMF
[15]	2014	94.70	93.80	92.20	94.80	-	-	-	-
[16]	2014	-	-	-	-	1.453	1.328	1.247	1.063
[7]	2010	-	-	-	-	1.78	1.73	1.44	1.64
[17]	2014	-	-	-	-	0.15	0.26	0.20	0.24
[18]	2013	95.54	94.33	95.93	96.72	0.384	0.54	0.781	0.354
[19]	2014	-	-	-	-	0.29	0.267	0.284	0.25
[20]	2011	-	-	-	-	1.650	1.610	1.326	1.097
[21]	2015	-	-	-	-	1.009	1.077	0.740	1.0615
[4]	2014	90.30	88.68	89.79	89.79	-	-	-	-
[22]	2011	88.59	89.90	89.49	88.48	-	-	-	-
[23]	2011	86.43	86.58	85.89	86.16	-	-	-	-
[14]	2011	-	-	-	-	0.43	1.02	0.95	0.91
Our paper	-	99.60	99.19	99.39	100.00	0.10	0.10	0.11	0.00

*LMF, LIF, RIF and RMF in %

Experiment 3: The goal of this experiment is to investigate the system's performance in the case of information fusion.

Table.4. EER/ROR (%) obtained by the fusion of the different fingers types

EER/ROR	Fusion of Two Types Fingers											
	LIF-LMF		LMF-RMF		LMF-RIF		RIF-RMF		LIF-RIF		RMF-LIF	
	EER	ROR	EER	ROR	EER	ROR	EER	ROR	EER	ROR	EER	ROR
Sum rule	0	99.8	0	99.9	0.08	99.8	0.01	99.7	0	100	0	99.9
Min rule	0.01	99.7	0	99.8	0.1	99.6	0.10	99.6	0	99.9	0.02	99.49
Max rule	0.10	99.49	0.01	99.9	0.1	99.6	0.02	99.6	0	100	0	99.8
Concatenation	0	99.9	0	99.9	0	99.9	0.00	99.8	0	100	0	100

EER/ROR	Fusion of Three or all Types Fingers									
	LMF-LIF-RIF		LMF-LIF-RMF		RMF-RIF-LMF		RMF-RIF-LIF		All Fingers	
	EER	ROR	EER	ROR	EER	ROR	EER	ROR	EER	ROR
Sum rule	0	100.00	0	100.00	0	99.90	0	100	0	100
Min rule	0.01	99.60	0.10	99.09	0.10	99.39	0.01	99.29	0.11	98.89
Max rule	0	99.60	0	99.90	0.09	99.60	0.08	99.80	0.08	99.8
Concatenation	0	100.00	0	100.00	0	100.00	0	100	0.00	100

*EER, ROR in %

For the purpose of this experiment, the information presented by the different finger types (LIF, LMF, RIF and RMF modality) of each person is fused. In other words, it is possible to concatenate these features into a single feature for each user. Also, these features are subjected to subspace projection PCA+LDA. In the proposed system, different combinations of finger types were tested to find the combination that optimizes the system accuracy. Thus, several tests are performed and the results are illustrated Table.4, which manifests that the fusion strategy can effectively improve the system performance.

However, a best error, EER=0% was obtained on mode verification and the highest recognition rate, Rank-1=100% on mode identification by fusing only two fingers type (LIF and RIF) using concatenation or sum rule. Thus, finally, a comparison of our multimodal system with the other state-of-the-art systems is presented in the Table.5. A comparison of ERR between the mode verification of the proposed system and that of [7], [19], and [21] reveals that the proposed system has the lowest EER. In comparison to the mode identification of the Rank-1 of other systems [18] [22] and [4], the proposed system provides the highest recognition rate.

Table.5. Comparative of proposed multimodal system with the existing approaches for FKP

References		LIF-RIF	LIF-LMF	Four fingers
[7]	EER (%)	0.26	0.20	0
	Rank-1	-	-	-
[19]	EER (%)	0.162	0.125	0
	Rank-1 (%)	-	-	-
[21]	EER (%)	0.08	0.04	0
	Rank-1 (%)	-	-	-
[18]	EER (%)	0.162	0.125	0
	Rank-1 (%)	98.69	99.09	100
[22]	EER (%)	-	-	-
	Rank-1 (%)	95.25	95.56	96.56
[4]	EER (%)	-	-	-
	Rank-1 (%)	97.27	95.55	99.29
[24]	Rank-1 (%)	98.08	98.69	100
[25]	EER (%)	0	0.09	0
	Rank-1 (%)	100	99.8	100
Proposed Work	EER (%)	0	0	0
	Rank-1 (%)	100	99.9	100

*LIF-RIF, LIF-LMF, Four fingers in %

4. CONCLUSIONS

As enumerated by the preceding sections, this paper has presented a new LGBSIF descriptor for constructing an efficient biometric based personal recognition system. For this purpose, the 1D-Log-Gabor filter is employed to generate the real and imaginary parts from FKP images. Each part thus obtained is encoded with BSIF descriptor, and the histograms extracted from the encoded real and imaginary images are concatenated into a large feature vector. The PCA+LDA technique is then used to reduce the dimensionality of this feature; and the nearest neighbor classifier that is based on Cosine distance is used for the recognition phase.

From the experimental results obtained from a data-base of 165 persons, the performance efficiency of the proposed system is inferred to be very encouraging. This also indicates that FKP modality can convincingly cater to the requirements of biometric security systems.

It is observed that the usage of multiple finger types yields better results when compared to the use of single finger. Moreover, the extensive experiments demonstrate that the introduced method achieves significantly higher accuracy than the other state-of-the-art systems. Further experiments conducted on various databases also demonstrate that LGBSIF is a powerful texture descriptor.

Focusing future works on the integration of this modality with security systems that use other biometrics like fingerprint and/or palm-print shall certainly improve performance efficiency and ensure high accuracy.

REFERENCES

[1] A.K. Jain, P. Flynn and A. Ross, "*Handbook of Biometrics*", Springer, 2007.

[2] L. Zhang, L. Zhang, D. Zhang and H. Zhu, "Ensemble of Local and Global Information for Finger-Knuckle-Print Recognition", *Pattern Recognition Letters*, Vol. 44, No. 9, pp. 1990-1998, 2011.

[3] Z.S. Shariatmadar and K. Faez, "An Efficient Method for Finger-Knuckle-Print Recognition by using the Information Fusion at Different Levels", *Proceedings of IEEE International Conference on Hand-Based Biometrics*, pp. 1-6, 2011.

[4] B. Zeinali, A. Ayatollah and M. Kakooei, "A Novel Method of Applying Directional Filter Bank (DFB) for Finger-Knuckle-Print (FKP) Recognition", *Proceedings of 22nd Iranian Conference on Electrical Engineering*, pp. 500-504, 2014.

[5] M. Chaa, N.E Boukezzoula, A. Meraoumia and M. Korichi, "An Efficient Biometric based Personal Authentication System using Finger Knuckle Prints Features", *Proceedings of IEEE International Conference on Information Technology for Organizations Development*, pp. 1-5, 2016.

[6] A. Meraoumia, S. Chitroub and A. Bouridane, "Palm-Print and Finger-Knuckle-Print for Efficient Person Recognition based on Log-Gabor Filter Response", *Analog Integrated Circuits and Signal Processing*, Vol. 69, pp.17-27, 2011.

[7] L. Zhang, L. Zhang, D. Zhang and H. Zhu, "Online Finger-Knuckle-Print Verification for Personal Authentication", *Pattern Recognition Letters*, Vol. 43, No. 7, pp. 2560-2571, 2010.

[8] D.J. Fiel, "Relations between the Images and the Response Properties of Cortical Cells", *Journal of the Optical Society of America A*, Vol. 4, No. 12, pp. 2379-2394, 1987.

[9] J. Kannala and E. Rahtu, "BSIF: Binarized Statistical Image Features", *Proceedings of IEEE International Conference*

on International Conference on Pattern Recognition, pp. 1363-1366, 2012.

[10] M. Turk and A. Pentland, "Eigenfaces for Recognition", *Journal Cognitive Neuro-Science*, Vol. 3, No. 1, pp. 71-86, 1991.

[11] P.N. Belhumeur, J.P. Hespanha and D.J. Kriegman, "Eigenfaces vs. Fisherfaces: Recognition using Class Specific Linear Projection", *IEEE Transactions on Pattern Analysis and Machine Intelligence*, Vol. 19, No. 7, pp. 711-720, 1997.

[12] A. Hadid, J. Ylioinas and M. B. Lopez, "Face and Texture Analysis using Local Descriptors: A Comparative Analysis", *Proceedings of IEEE International Conference on Image Processing Theory, Tools and* Applications, pp. 1-4, 2014.

[13] D. Zhang, X. Jing and J. Yang, "*Biometric Image Discrimination Technologies: Computational Intelligence and its Applications Series*", IGI Global, 2006.

[14] E. Morales, C.M. Travieso, M.A. Ferrer and J.B. Alonso, "Improved Finger-Knuckle-Print Authentication based on Orientation Enhancement", *Electronics Letters*, Vol. 47, No. 6, pp. 380-381, 2011.

[15] W. El-Tarhouni, M.K. Shaikh, L. Boubchir and A. Bouridane, "Multi-Scale Shift Local Binary Pattern Based-Descriptor for Finger-Knuckle-Print Recognition", *Proceedings of 26th International Conference on Microelectronics*, pp. 184-187, 2014.

[16] G. Gao, J. Yang, J. Qian and L. Zhang, "Integration of Multiple Orientation and Texture Information for Finger-Knuckle-Print Verification", *Neuro Computing*, Vol. 135, pp. 180-191, 2014.

[17] T. Kong, G. Yang and L. Yang, "A Hierarchical Classification Method for Finger Knuckle Print Recognition", *EURASIP Journal on Advances in Signal Processing*, Vol. 4, pp. 1-8, 2014.

[18] Z.S. Shariatmadar and K. Faez, "Finger Knuckle Print Recognition Via Encoding Local-Binary-Pattern", *Journal of Circuits, Systems, and Computers*, Vol. 22, No. 6, pp. 1-6, 2013.

[19] Z.S. Shariatmadar and K. Faez, "Finger-Knuckle-Print Recognition Performance Improvement Via Multi-Instance Fusion at the Score Level", *Optik*, Vol. 125, No. 3, pp. 908-910, 2014.

[20] M. Xiong, W. Yang and C. Sun, "Finger-Knuckle-Print Recognition using LGBP", *Proceedings of International Symposium on Neural Networks*, pp. 270-277, 2011.

[21] A. Nigam, K. Tiwari and P. Gupta, "Multiple Texture Information Fusion for Finger-Knuckle-Print Authentication System", *Neurocomputing*, Vol. 188, pp. 190-205, 2016.

[22] Z.S. Shariatmadar and K. Faez, "An Efficient Method for Finger Knuckle- Print Recognition by using the Information Fusion at Different Levels", *Proceedings of International Conference on Hand-Based Biometrics*, pp. 1-6, 2011.

[23] X. Jing, W. Li, C. Lan, Y. Yao, X. Cheng and L. Han, "Orthogonal Complex Locality Pre-Serving Projections based on Image Space Metric for Finger-Knuckle-Print Recognition", *Proceedings of International Conference on Hand-Based Biometrics*, pp. 1-6, 2011.

[24] M. Chaa, N.E. Boukezzoula and A. Meraoumia, "Features-Level Fusion of Reflectance and Illumination Images in Finger-Knuckle-Print Identification System", *International Journal on Artificial Intelligence Tools*, Vol. 27, No. 3, pp. 1-16, 2018.

[25] A. Attia, M Chaa, Z. Akhtar and Y. Chahir, "Finger Kunckcle Patterns based Person Recognition via Bank of Multi-Scale Binarized Statistical Texture Features", *Evolving Systems*, Vol. 92, pp. 1-11, 2018.